Optik - International Journal for Light and Electron Optics 241 (2021) 166944

Contents lists available at ScienceDirect

Optik

journal homepage: www.elsevier.com/locate/ijleo

Original research article

Site occupancy and phonon sideband of trivalent europium doped calcium aluminosilicate phosphors

Nguyen Thi Quynh Lien [a], Ho Van Tuyen [b,c], Nguyen Ha Vi [b,c], A.N.H. Thuan [d], Phan Van Do [e,*]

[a] Faculty of Basic Sciences, Van Lang University, 45 Nguyen Khac Nhu street, Co Giang ward, District 1, Ho Chi Minh city, Viet Nam
[b] Institute of Research and Development, Duy Tan University, Da Nang, 550000, Viet Nam
[c] Faculty of Natural Sciences, Duy Tan University, Da Nang, 550000, Viet Nam
[d] NTT Hi-Tech Institute, Nguyen Tat Thanh University, Ho Chi Minh city, Viet Nam
[e] Thuyloi University, 175 Tay Son, Dong Da, Hanoi, Viet Nam

ARTICLE INFO

Keywords:
Phonon sideband
Solid-state reaction
Site occupancy
Aluminosilicate

ABSTRACT

A series of Eu^{3+} doped $Ca_2Al_2SiO_7$ were synthesized by the solid-state reaction method. Structural and luminescent properties of the obtained samples were investigated through X-ray diffraction, Raman and luminescence spectra. The luminescent characteristic of the $^5D_0 \rightarrow {}^7F_{0,1}$ transitions from emission spectra of Eu^{3+} ions showed that the Eu^{3+} ions occupy at two different sites in $Ca_2Al_2SiO_7$ lattice. The $Ca_2Al_2SiO_7$:Eu^{3+} red phosphors have three phonon sidebands with energies ~673 cm^{-1}, 848 cm^{-1} and 1443 cm^{-1} which have been determined via the excitation spectra of Eu^{3+} ions in $Ca_2Al_2SiO_7$ materials. These obtained phonon energies coincided with the vibrational energies observed from Raman spectra. The multiphonon relaxation rates for the excited levels of $^5D_1$, $^5D_2$ and $^5D_3$ of Eu^{3+} ions in $Ca_2Al_2SiO_7$ were also calculated.

1. Introduction

Silicate-based phosphors such as $M_3MgSi_2O_8$ (M: Ba, Ca, Sr) [1], $Sr_2MgSi_2O_7$ [2], $M_2Al_2SiO_7$ (M: Sr, Ca) [3,4] have been used as a good host for luminescent materials due to their high chemical stability and water-resistance properties [2,4,5]. In particular, calcium aluminosilicate (CAS:$Ca_2Al_2SiO_7$) doped with rare earth (RE) ions is an interesting phosphor and has been studied for white light-emitting diodes [5–7], laser [8,9], piezo-electrification [7,10] and applications in thermoluminescence [7,10,11]. In this direction, CAS doping with Eu^{3+} ions is used as a red emission phosphor for white light-emitting diodes (white-LEDs) to yield a high color reproducibility and a high color rendering index [12]. Furthermore, the effect of compensator (Na, Al) on optical properties of $Ca_2Al_2SiO_7$:Eu^{3+} phosphors [13], adjustable double center emission of Eu^{3+} and Eu^{2+} co-doped $Ca_2Al_2SiO_7$ [14], energy transfer from Pb^{2+} or Bi^{3+} to Eu^{3+} in $Ca_2Al_2SiO_7$ [15,16] have also studied and reported. In the structure of CAS, cations has found on three types of sites: eightfold coordinated sites occupied by Ca^{2+} ions and two types of tetrahedral sites (T1, and T2) for Al^{3+} and Si^{4+} ions [6,9] and when RE ions are doped into CAS lattice, they substitute Ca^{2+} ions in the eightfold coordinated sites [9]. Several studies have shown that luminescence of Eu^{3+} ions is affected by the number of site occupancy of Eu^{3+} in host lattice: C. G. Liu [17] and J. Zhou [18] reported that Eu^{3+} ions occupy at two different sites in $12CaO.7Al_2O_3$ powders and in $Na_3LuSi_3O_9$ phosphor, respectively and the luminescence of these phosphors is a sum of emissions of Eu^{3+} at two sites. Yanlin Huang et al., have shown three different sites of Eu^{3+}

* Corresponding author.
E-mail address: phanvando@tlu.edu.vn (P.V. Do).

https://doi.org/10.1016/j.ijleo.2021.166944
Received 7 March 2021; Accepted 12 April 2021
Available online 18 April 2021

ions in $EuBaB_9O_{16}$ phosphor and two of them are due to the presence of structural defects in the vicinity of Eu^{3+} dopants, they affect to the Eu^{3+} luminescence because of modifying the local symmetry [19]. However, the phonon energy and site occupancy of Eu^{3+} of such CAS phosphors have not been investigated systematically. Since the materials with low phonon energy gives the stronger luminescence of Eu^{3+} ions in which non-radiative transition rates are decreased, thus Eu^{3+} -doped luminescence phosphor plays an important role in developing the high quality white-LEDs. Therefore, the aim of the present work is to study the site occupancy of Eu^{3+} ions and the phonon energy in $Ca_2Al_2SiO_7$ materials. The site occupancy of Eu^{3+} in CAS lattice was estimated by the analysis of its emission spectra. The phonon sideband was determined by excitation spectra of Eu^{3+} in CAS and the electron–phonon coupling constant and the multiphonon relaxation rate were also estimated via phonon sideband analysis.

2. Experiments

2.1. Materials preparation

Powder samples $Ca_2Al_2SiO_7$:*x*. Eu^{3+} (x = 0.5, 1.0, 2.0 and 3.0 mol%) have been synthesized by the solid-state reaction method. The starting materials were $CaCO_3$ (AR), Al_2O_3 (AR), SiO_2 (Sigma), and Eu_2O_3 (Merck). First step, initial materials were weighed according to their nominal compositions and mixed homogeneously for 2 h. After that the obtained mixture was calcined in air from room temperature to 1280 °C with temperature rate of 200 °C/1 h and annealed at 1280 °C for 1 h. In final step, it was cooled to room temperature to obtain a product of white powder. The name of the obtained samples is denoted as E05, E10, E20, and E30 corresponding to dopant concentrations of 0.5, 1.0, 2.0 and 3.0 mol%, respectively.

2.2. Characterization

The crystalline structures of the prepared phosphors have analyzed using by a X-ray diffractometer (D8-Advance; Bruker, Germany) with Cu Kα radiation (λ = 0.154 nm). Raman spectra of the samples have been recorded by Xplora-Plus equipment (Horiba Jobin-Yvon). The photoluminescence (PL) and photoluminescence excitation (PLE) spectra were measured at room temperature by using a spectrophotometer (FL3–22; Horiba Jobin-Yvon) with Xenon - 450 W lamp as an excited source.

3. Results and discussion

3.1. X-ray diffraction, SEM image and Raman spectra results

A series of XRD patterns of $Ca_2Al_2SiO_7$:*x*. Eu^{3+} (x = 0.5, 1.0, 2.0 and 3.0 mol%) are presented in Fig. 1. The XRD patterns of all the samples are similar and the characterized diffraction peaks coincide with the standard profile of $Ca_2Al_2SiO_7$ (JCPDS No. 35-0755). The prepared samples are all of a single phase of $Ca_2Al_2SiO_7$ with tetragonal structure and no impurity phases are observed indicating that small amount of dopant did not change the structure of host lattice.

Raman spectra in the 100–1100 cm^{-1} region of all the obtained samples were measured at room temperature using laser 532 nm and shown in Fig. 2. It showed that the Raman spectra of all the samples show similar nature in peak position with various

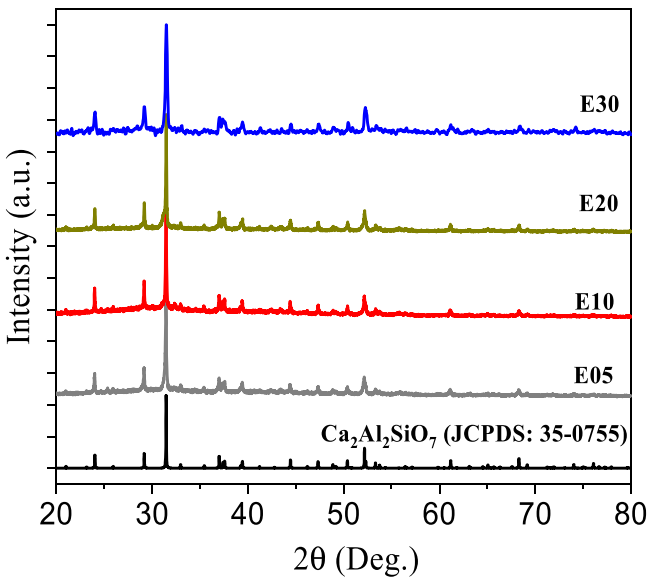

Fig. 1. XRD patterns of the prepared samples E05, E10, E20, and E30.

concentrations of Eu^{3+} ions. Two weak vibration peaks at 238 cm^{-1} and 300 cm^{-1} are due to the lattice modes and the strongest peak observed at 625 cm^{-1} is attributed to the stretching modes of the T-O-T bonds (T = Si or Al) [3,12]. The vibrations observed at 662 cm^{-1} and 800 cm^{-1} are assigned to the stretching modes of the AlO_4 tetrahedral [3], and peaks at 913 cm^{-1} and 970 cm^{-1} correspond to the symmetric stretching of the pyrosilicate group ($Si–O^-$) [3,12].

3.2. Excitation spectra and phonon sideband analysis

The photoluminescence excitation spectra monitored at the emission wavelength of 617 nm for all the samples presented in Fig. 3 (a) have the same shape with a strong broad band around 260 nm and many sharp peaks in the 300–480 nm region. The strong broad band centered around 260 nm is assigned to the charge transfer band from O^{2-} to Eu^{3+}, while the sharp peaks are due to the 4f-4f excited transitions of Eu^{3+} ions in CAS material. Intensity of excitation spectra increases with the increasing of dopant concentration due to the increasing of the Eu^{3+} luminescence center in host lattice. As can be seen in Fig. 3(a), several strong excitation transitions of Eu^{3+} ion in CAS material include of the $^7F_0 \rightarrow {}^5H_6$ transition (318 nm), $^7F_0 \rightarrow {}^5D_4$ (361 nm), $^7F_0 \rightarrow {}^5G_4$ (380 nm), $^7F_0 \rightarrow {}^5L_6$ (392 nm), $^7F_0 \rightarrow {}^5D_3$ (412 nm), $^7F_0 \rightarrow {}^5D_2$ (463 nm), in which the strongest intensity corresponds to the $^7F_0 \rightarrow {}^5L_6$ transition.

Among the 4f-4f transitions of Eu^{3+} ions, the $^7F_0 \rightarrow {}^5D_2$ excited transition is usually chosen to evidence the phonon sidebands (PSB) since energy difference between $^5D_2$ level and the next upper level $^5D_3$ is large (2500 cm^{-1}) [20] and there is no energy levels between them. Therefore, any small peaks at the higher energy side of pure electronic transition $^7F_0 \rightarrow {}^5D_2$ could not be assigned as electronic transition and are often referred as phonon sideband. It is observed in inset of Fig. 3(a) that the samples have three PSB which were centered at 449.0 nm (P1), 446.0 nm (P2), and 434.5 nm (P3). The energy difference between zero phonon line (ZPL) and a PSB is referred as phonon energy ($\hbar\omega$). The phonon energies for E10 sample are presented in Fig. 3(b) and value of $\hbar\omega$ for all the samples are listed in Table 1. The phonon energy of peak P3 for all samples reaches value in the1393 cm^{-1}–1443 cm^{-1} region, which is related to the Si–O–H vibration [21]. While the phonon energies of peaks P1 (625 cm^{-1}–673 cm^{-1}) and P2 (833 cm^{-1}–850 cm^{-1}) are very close to vibrations at 662 cm^{-1} and 800 cm^{-1} relating to the stretching modes of the AlO_4 tetrahedra as mentioned in the Raman spectra in the Section 3.1. The electron-phonon coupling factor *g* is defined as a ratio of the intensity of PSB and of the pure-electron transition (PET) $^7F_0 \rightarrow {}^5D_2$ of Eu^{3+} ions. Value of *g* for all the prepared samples were calculated and also shown in Table 1, it changes from 0.067 to 0.098 with the Eu^{3+} different concentrations. Results of PSB energy and *g* values showed that there is no tendency of PSBs with increasing dopant concentration. Hence, we only chose the E10 sample as a represent to calculate the multiphonon relaxation rate for each phonon sidebands in next paragraph.

Under excitation of 392 nm, Eu^{3+} ions were excited to the $^5L_6$ excited level but its emissions are transitions from the $^5D_0$ lowest excited level. The emission intensity from $^5D_0$ to ^7F_J depends to the population at $^5D_0$ level, it relates to multiphonon relaxation from the $^5L_6$ excited level. In CAS host lattice, because of the large phonon energy (1443 cm^{-1}) the energy gap between $^5L_6$ and $^5D_0$ levels is bridged easy and the multiphonon relaxation process is accelerated. Therefore, Eu^{3+} ions quickly change from the excited level $^5L_6$ to the lowest excited level $^5D_0$ where it emits the emission transition to ^7F_J levels. In addition, since Eu^{3+} ions quickly relax to $^5D_0$ level, the emission transitions from other ^5D_J ($^5D_1$,$^5D_2$,...) levels can be ignored and ensure a better red emission of Eu^{3+} ions in CAS material. The partial energy level diagram of Eu^{3+} ions in CAS material including the multiphonon relaxation process is given in Fig. 4. According to Miyakawa and Dexter, the probability of the non-radiative decay rate through the multiphonon relaxation is given by the following equation [22–24]:

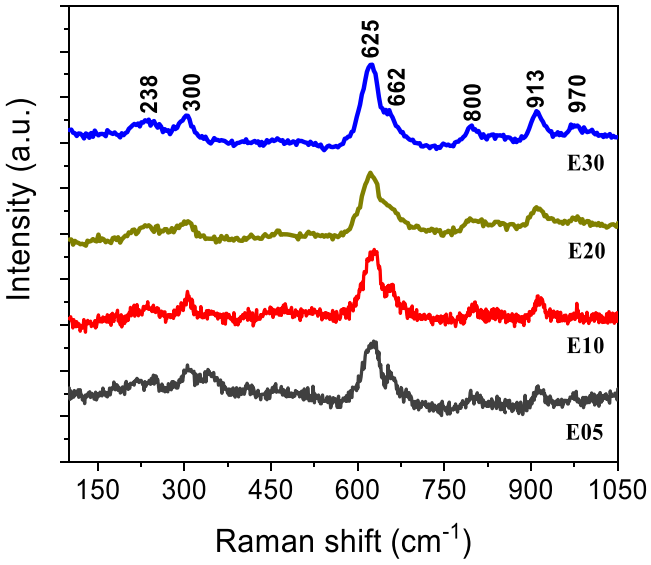

Fig. 2. Raman spectra of the prepared samples E05, E10, E20, and E30.

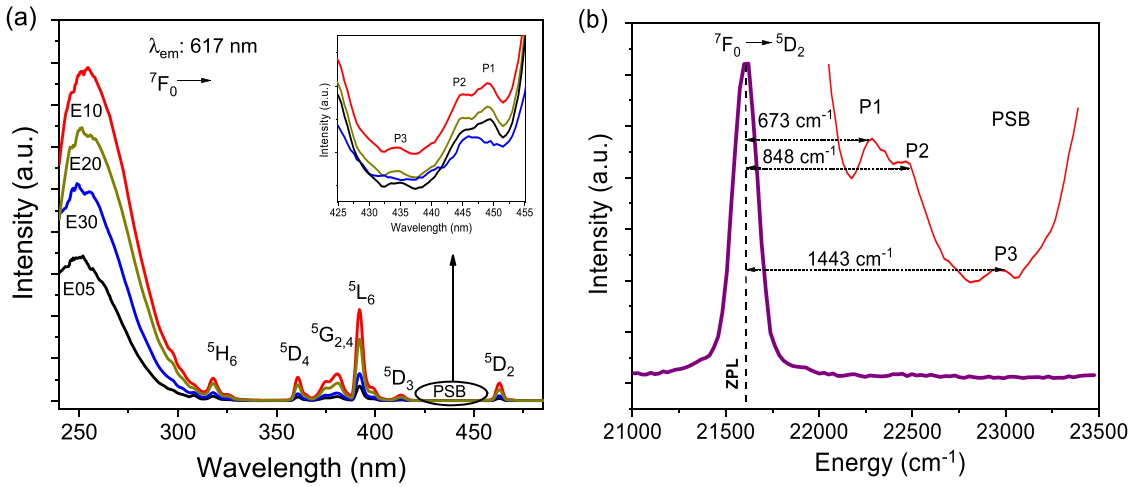

Fig. 3. PLE spectra of all the prepared samples (a) and PSBs of E10 sample (b).

Table 1
The phonon energies ($\hbar\omega$) and electron-phonon coupling factor (g).

Samples	$\hbar\omega$ (cm^{-1})			g
	P1	P2	P3	
E05	650	850	1393	0.098
E10	673	848	1443	0.077
E20	625	825	1420	0.067
E30	673	823	1417	0.082

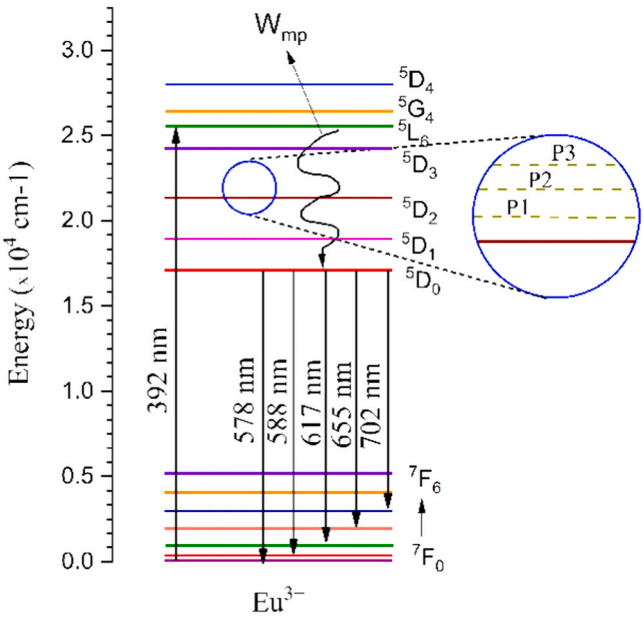

Fig. 4. Partial energy level diagram showing the phonon sideband in CAS:Eu^{3+} phosphor.

$$W_{mp} = W_0.\exp(-\alpha.\Delta E) \quad (1)$$

Where W_0 is the decay rate at zero energy gap and zero phonon emission, ΔE is the energy gap from the $^5D_1$, $^5D_2$, $^5D_3$ excited levels to the next lower energy level. α is the host dependent parameter and it is given by:

$$\alpha = (\hbar\omega)^{-1}\left[\ln\left(\frac{p}{g(n+1)}\right) - 1\right] \quad (2)$$

Where p is the number of phonon required to bridge the energy gap ΔE, and n is the partition distribution function, which can be expressed as bellow:

$$p = \frac{\Delta E}{\hbar\omega} \quad (3)$$

$$n = \left(e^{\hbar\omega/kT} - 1\right)^{-1} \quad (4)$$

Where k is the Boltzmann constant. At room temperature, $kT = 208.5$ cm^{-1}, the energy gaps between the $^5D_1$, $^5D_2$ and $^5D_3$ levels and the next lower level are found to be 1789 cm^{-1}, 2479 cm^{-1} and 2674 cm^{-1} for E10 sample, respectively. From these values, phonon sideband parameters of the E10 sample are determined and presented in Table 2. Above equations indicates that the multiphonon relaxation rate (W_{mp}) decreases with increase of the energy gap (ΔE) and the higher number of phonons (p). As can be seen in Table 2, the number of phonon changes from 1.2 to 1.9 for the large phonon energy (P3) and from 2.1 to 4.0 for the small phonon energy (P1 and P2), this leads to the relative multiphonon relaxation rate (W_{mp}/W_0) increases for phonon sideband P3. Comparison to other materials, the relative multiphonon relaxation rate (W_{mp}/W_0) of CAS is the same order of magnitude with that of SiO_2-TiO_2-PDMS (5410×10^{-5}) [25] but larger than that of $BaGd_2ZnO_5$ (1.67×10^{-8}) [20]. Because of high relaxation rate, the luminescence from the high excited levels $^5D_1$, $^5D_2$ and $^5D_3$ of Eu^{3+} ions is quickly quenched and the obtained emission is dominated by the $^5D_0 \rightarrow {}^7F_J$ transitions with a better red emission of Eu^{3+} ions in CAS material comparing to $BaGd_2ZnO_5$ oxide.

3.3. Luminescence properties and analysis of the site occupancy of Eu^{3+} in CAS host lattice

In this section, we used the luminescent characteristic of the $^5D_0 \rightarrow {}^7F_0$ and $^5D_0 \rightarrow {}^7F_1$ transitions obtained from the photoluminescence (PL) spectra to evaluate number of site occupancy of Eu^{3+} ions in CAS host lattice. The PL spectra of Eu^{3+} ions in CAS samples using excitation radiation of 392 nm presented in Fig. 5 include of sharp peaks in the 560–720 nm region, which are results from the $^5D_0 \rightarrow {}^7F_J$ ($J = 0, 1,..., 4$) transitions. In which, the emission peak at 617 nm ($^5D_0 \rightarrow {}^7F_2$) has the strongest intensity and it is dominant contribution for red emission of CAS:Eu^{3+} phosphor. As can be seen, emission intensity changes with the Eu^{3+} ion concentrations and has been found to be quenched at 1 mol% of Eu^{3+} ions due to the concentration quenching phenomenon.

Among the $^5D_0 \rightarrow {}^7F_J$ ($J = 0, 1,..., 6$) transitions of Eu^{3+} ions, the $^5D_0 \rightarrow {}^7F_1$ transition is a magnetic dipole and usually used as a reference transition because its intensity is not considerably affected by the crystal field. While the $^5D_0 \rightarrow {}^7F_2$ transition is an allowed electric dipole, and is strongly affected by the change of the Eu^{3+} surroundings [26]. Therefore, the ratio (R) of the intensity of the $^5D_0 \rightarrow {}^7F_2$ transition to that of the $^5D_0 \rightarrow {}^7F_1$ transition can be used to evaluate the surrounding environment of the Eu^{3+} site. Several literatures have indicated that the R value has been found to decrease with the increase of Eu–O ionicity [27,28]. The R value was found to be 1.71, 1.94, 1.96 and 2.00 corresponding to E05, E10, E20 and E30 samples, it increases with high Eu^{3+} concentration. This increase has also observed for $BaGd_2ZnO_5$:Eu phosphor, in which the increase of R value with europium concentration is due to the expansion of the host lattice when europium content increased [20]. Besides that, these R values of CAS phosphor are smaller than that of the strontium aluminosilicate phosphors ($Sr_2Al_2SiO_7$:Eu^{3+}, $R = 2.25$) [29] indicating the ionicity of the Eu–O bond in $Ca_2Al_2SiO_7$ comparison to $Sr_2Al_2SiO_7$ material.

The $^5D_0 \rightarrow {}^7F_0$ transition has maximum one peak in emission spectra for a single Eu^{3+} site due to the non-degeneracy of both $^7F_0$ and $^5D_0$ levels, therefore, this transition can be used as an useful tool to determine the number of the Eu^{3+} sites in host lattices [18,26]. Generally, Eu^{3+} will occupy one site in host lattice, however it can be occupied at more than one site in several materials such as two sites in $Na_3LuSi_3O_9$ [18], $Mg_2Al_4Si_5O_{18}$ [30], $12CaO.7Al_2O_3$ materials [17] three sites in $EuBaB_9O_{16}$ phosphor [19] and four sites in

Table 2
The electron-phonon coupling factor g, number of phonon n, α parameter and the relative multiphonon relaxation rate (W_{mp}/W_0) of E10 sample.

$\hbar\omega$ (cm^{-1})	g	*Levels*	p	α (x 10^{-3} cm)	W_{mp}/W_0 (x 10^{-5})
P1 (673 cm^{-1})		$^5D_1$	2.7	5.1	10.32
	0.030	$^5D_2$	3.7	5.6	0.10
		$^5D_3$	4.0	5.7	0.02
P2 (848 cm^{-1})	0.028	$^5D_1$	2.1	3.9	98.11
		$^5D_2$	2.9	4.3	2.61
		$^5D_3$	3.2	4.3	0.90
P3 (1443 cm^{-1})	0.019	$^5D_1$	1.2	2.2	1195
		$^5D_2$	1.7	2.4	245
		$^5D_3$	1.9	2.5	133

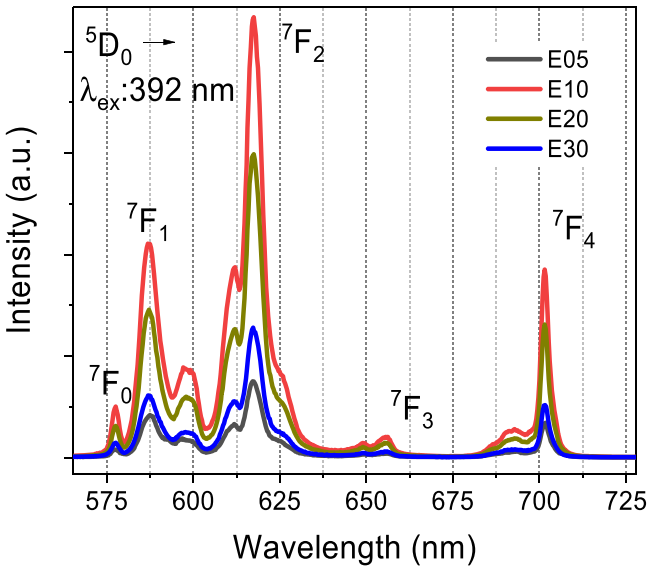

Fig. 5. PL spectra of the prepared samples E05, E10, E20, and E30. (For interpretation of the references to colour in this figure, the reader is referred to the web version of this article.)

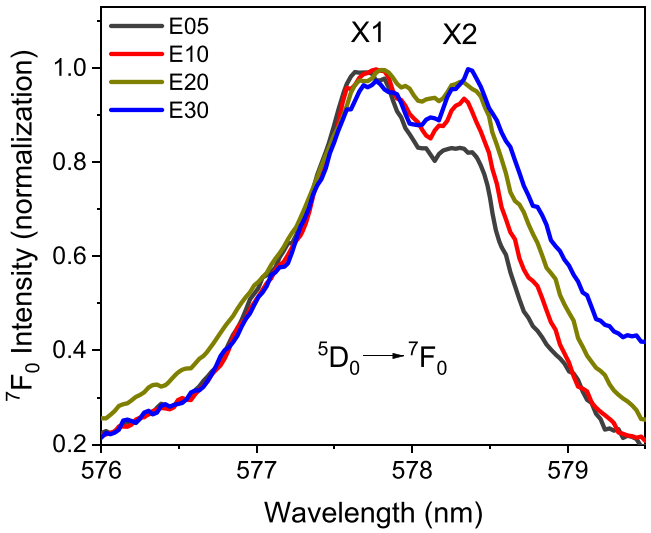

Fig. 6. Intensity variation of the $^5D_0 \rightarrow {}^7F_0$ transition of Eu^{3+} ions in CAS materials.

yttrium aluminum garnet [31]. In our case, the $^5D_0 \rightarrow {}^7F_0$ transition is observed two peaks in the 576–580 nm region of emission spectra of all the obtained samples, they are labeled by X1 (577.7 nm) and X2 (578.4 nm) as presented in Fig. 6. Therefore, we suggested that the Eu^{3+} ions probably located in two different sites in the CAS lattices. The first site of the Eu^{3+} ions in the $Ca_2Al_2SiO_7$ lattice is expected to occupy at Ca^{2+} site because the ionic radii of Eu^{3+} ions (107 pm) is close to that of Ca^{2+} ions (112 pm) [13]. While the ion radius of Al^{3+} (39 pm) and Si^{4+} (26 pm) are too small for Eu^{3+} ions occupy, hence the second site for Eu^{3+} ions is maybe the interstitial site in host lattice [32]. Besides that, intensity of emission peak at X2 was weak at low Eu^{3+} concentration and become stronger with increasing Eu^{3+} content indicating amount of Eu^{3+} ions occupying at X2 site rise at the high dopant concentrations. Another evidence of the existence of two different sites of Eu^{3+} ions in the CAS host lattice is the split of the $^5D_0 \rightarrow {}^7F_1$ emission transition, which is splitted into five peaks locating around 586 nm, 588 nm, 593 nm, 597 nm and 601 nm as observed in Fig. 7. It is known that the $^5D_0 \rightarrow {}^7F_1$ ($J = 1$) is a magnetic transition and it will show maximum three emission peaks or two emission peaks if Eu^{3+} occupies at a site with low symmetry and only one emission peak if Eu^{3+} locates at the site with high symmetry as T_h and O_h point group symmetry [17,18]. Therefore, in our case, the presence of five emission peaks belong to the $^5D_0 \rightarrow {}^7F_1$ transition indicating that there are more than one site of Eu^{3+} ions in CAS lattice. This result confirms for suggestion of two Eu^{3+} different sites in the CAS lattice as mentioned above.

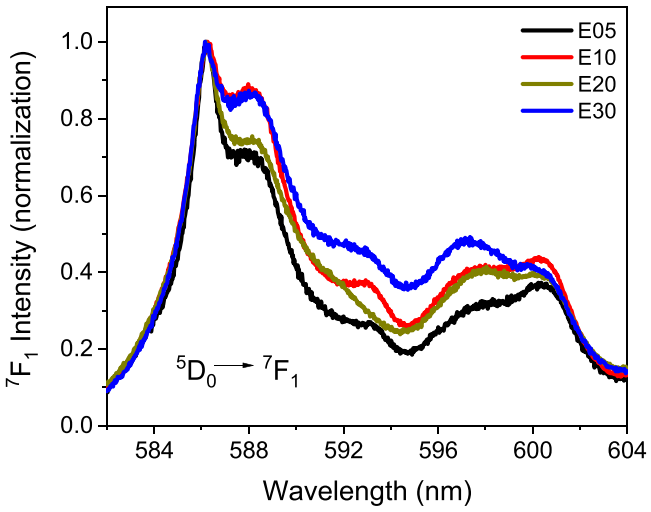

Fig. 7. Intensity variation of the $^5D_0 \rightarrow {}^7F_1$ transition of Eu^{3+} ions in CAS materials.

4. Conclusions

The red emission phosphor $Ca_2Al_2SiO_7:Eu^{3+}$ was successfully synthesized by the solid state reaction at 1280 °C and achieved a single phase of $Ca_2Al_2SiO_7$ with tetragonal structure. Vibrational modes for $Ca_2Al_2SiO_7:Eu^{3+}$ phosphor were observed through Raman spectra with intense vibrations at 625 cm^{-1}, 800 cm^{-1}, 913 cm^{-1}, 970 cm^{-1}. Results from PLE spectra showed all the prepared samples have three phonon sidebands, which associated with the $^5D_0 \rightarrow {}^7F_2$ transition of Eu^{3+} ions and their phonon energies are found to be ~673 cm^{-1}, 848 cm^{-1} and 1443 cm^{-1}. Two emission peaks belonging the $^5D_0 \rightarrow {}^7F_0$ transition in PL spectra showed that there are two different site occupancy of Eu^{3+} ions in $Ca_2Al_2SiO_7$ phosphor, and it was also confirmed by observation on the $^5D_0 \rightarrow {}^7F_1$ transition.

Declaration of Competing Interest

The authors declare that they have no known competing financial interests or personal relationships that could have appeared to influence the work reported in this paper.

References

[1] Y. Yonesaki, T. Takei, N. Kumada, N. Kinomura, Crystal structure of Eu^{2+}-doped $M_3MgSi_2O_8$ (M: Ba, Sr, Ca) compounds and their emission properties, J. Solid State Chem. 182 (2009) 547–554.
[2] F. Song, C. Donghua, Y. Yuan, Synthesis of $Sr_2MgSi_2O_7$:Eu, Dy and $Sr_2MgSi_2O_7$:Eu, Dy, Nd by a modified solid-state reaction and their luminescent properties, J. Alloy. Compd. 458 (2008) 564–568.
[3] M.A. Bouhifd, G. Gruener, B.O. Mysen, P. Richet, Premelting and calcium mobility in gehlenite ($Ca_2Al_2SiO_7$) and pseudowollastonite ($CaSiO_3$), Phys. Chem. Miner. 29 (2002) 655–662.
[4] W. Zhou, X. Ma, M. Zhang, Y. Luo, Z. Xia, Effect of different RE dopants on phosphorescence properties of $Sr_2Al_2SiO_7:Eu^{2+}$ phosphors, J. Rare Earths 33 (2015) 700–705.
[5] H. Jiao, G. Zhang, P. Wang, Q. Chen, L. Liu, C. Limao, Y. Wang, Crystal structure refinement, photoluminescence properties and energy transfer of multicolor tunable $Ca_2Al_2SiO_7:Tm^{3+}$, Dy^{3+} for NUV white-light-emitting diodes, Spectrochim. Acta Part A Mol. Biomol. Spectrosc. 229 (2020), 117942.
[6] H. Jiao, Y. Wang, $Ca_2Al_2SiO_7:Ce^{3+}$, Tb^{3+}: a white-light phosphor suitable for white-light-emitting diodes, J. Electrochem. Soc. 156 (2009) J117.
[7] G. Tiwari, N. Brahme, R. Sharma, D.P. Bisen, S.K. Sao, S.J. Dhoble, A study on the luminescence properties of gamma-ray-irradiated white light emitting $Ca_2Al_2SiO_7:Dy^{3+}$ phosphors fabricated using a combustion-assisted method, RSC Adv. 6 (2016) 49317–49327.
[8] P.L. Boulanger, J.-L. Doualan, S. Girard, J. Margerie, R. Moncorge, B. Viana, Excited-state absorption of Er^{3+} in the $Ca_2Al_2SiO_7$ laser crystal, J. Lumin. 86 (2000) 15–21.
[9] A.M. Lejus, A. Kahn-Harari, J.M. Benitez, B. Viana, Crystal growth, characterization and structure refinement of neodymium 3+ doped gehlenite, a new laser material [$Ca_2Al_2SiO_7$], Mater. Res. Bull. 29 (1994) 725–734.
[10] G. Tiwari, N. Brahme, R. Sharma, D.P. Bisen, S.K. Sao, S. Tigga, Luminescence properties of dysprosium doped di-calcium di-aluminium silicate phosphors, Opt. Mater. 58 (2016) 234–242.
[11] H. Wu, Y. Hu, G. Ju, L. Chen, X. Wang, Z. Yang, Photoluminescence and thermoluminescence of Ce^{3+} and Eu^{2+} in $Ca_2Al_2SiO_7$ matrix, J. Lumin. 131 (2011) 2441–2445.
[12] K. Park, H. Kim, D.A. Hakeem, Effect of host composition and Eu^{3+} concentration on the photoluminescence of aluminosilicate $(Ca,Sr)_2Al_2SiO_7:Eu^{3+}$ phosphors, Dyes Pigments 136 (2017) 70–77.
[13] Q. Zhang, J. Wang, M. Zhang, W. Ding, Q. Su, Enhanced photoluminescence of $Ca_2Al_2SiO_7:Eu^{3+}$ by charge compensation method, Appl. Phys. A 88 (2007) 805–809.
[14] Z. Xu, Y. Zhu, Q. Luo, Y. Pan, W. Wang, X. Liu, L. Li, Anomalous preparation, intense $^5D_0 \rightarrow {}^7F_4$ emission and adjustable double center emission of Eu^{3+} and Eu^{2+} codoped $Ca_2Al_2SiO_7$, Ceram. Int. 45 (2019) 20405–20413.
[15] X.H. Chuai, H.J. Zhang, F.S. Li, K.C. Chou, The luminescence of Eu^{3+} ion in $Ca_2Al_2SiO_7$, Opt. Mater. 25 (2004) 301–305.
[16] P. Yang, X. Yu, H. Yu, T. Jiang, X. Xu, Z. Yang, D. Zhou, Z. Song, Y. Yang, Z. Zhao, J. Qiu, $Ca_2Al_2SiO_7:Bi^{3+}$, Eu^{3+}, Tb^{3+}: a potential single-phased tunable-color-emitting phosphor, J. Lumin. 135 (2013) 206–210.

[17] C.G. Liu, Y.X. Liu, D. Wang, D.T. Yan, C.S. Xu, Characterization and luminescence of Eu^{3+} ions doped $12CaO{\cdot}7Al_2O_3$ nanopowders, J. Nanosci. Nanotechnol. 11 (2011) 9946–9952.
[18] J. Zhou, L. Xie, J. Zhong, H. Liang, J. Zhang, M. Wu, Site occupancy and luminescence properties of Eu^{3+} in double salt silicate $Na_3LuSi_3O_9$, Opt. Mater. Express 8 (2018) 736.
[19] Y. Huang, H. Lin, H.J. Seo, Luminescence properties and local structures of Eu^{3+} in $EuBaB_9O_{16}$ crystal, J. Electrochem. Soc. 157 (2010) J405.
[20] Ş. Georgescu, A. Enachi, O. Toma, Phonon sidebands of Eu^{3+} in $BaGd_2ZnO_5$, J. Lumin. 228 (2020), 117597.
[21] A.M. Efimov, V.G. Pogareva, A.V. Shashkin, Water-related bands in the IR absorption spectra of silicate glasses, J. Non Cryst. Solids 332 (2003) 93–114.
[22] T. Miyakawa, D.L. Dexter, Phonon sidebands, multiphonon relaxation of excited states, and phonon-assisted energy transfer between Ions in solids, Phys. Rev. B 1 (1970) 2961–2969.
[23] S. Gopi, S.K. Jose, A. George, N.V. Unnikrishnan, C. Joseph, P.R. Biju, Luminescence and phonon sideband analysis of Eu^{3+} doped alkali fluoroborate glasses for red emission applications, J. Mater. Sci. Mater. Electron. 29 (2017) 674–682.
[24] P. Manasa, C.K. Jayasankar, Luminescence and phonon side band analysis of Eu^{3+}-doped lead fluorosilicate glasses, Opt. Mater. 62 (2016) 139–145.
[25] M. Gopinath R. J, S. Gopi, S.M. Simon, A.C. Saritha, P.R. Biju, C. Joseph, N.V. Unnikrishnan, Spectroscopic analysis of Eu^{3+} doped silica–titania–polydimethylsiloxane hybrid ORMOSILs, RSC Adv. 10 (2020) 20057–20066.
[26] K. Binnemans, Interpretation of europium(III) spectra, Coord. Chem. Rev. 295 (2015) 1–45.
[27] S. Tanabe, S. Todoroki, K. Hirao, N. Soga, Phonon sideband of Eu^{3+} in sodium borate glasses, J. Non Cryst. Solids 122 (1990) 59–65.
[28] J.A. Capobianco, P.P. Proulx, M. Bettinelli, F. Negrisolo, Absorption and emission spectroscopy of Eu^{3+} in metaphosphate glasses, Phys. Rev. B 42 (1990) 5936–5944.
[29] H. Van Tuyen, D.T. Tien, N.M. Son, D. Van Phan, Judd–Ofelt parameters of Eu^{3+} and energy transfer of Ce^{3+}/Eu^{3+} in $Sr_2Al_2SiO_7$ materials, J. Electron. Mater. 48 (2019) 7799–7805.
[30] G.P. Thim, H.F. Brito, S.A. Silva, M.A.S. Oliveira, M.C.F.C. Felinto, Preparation and optical properties of trivalent europium doped into cordierite using the sol–gel process, J. Solid State Chem. 171 (2003) 375–381.
[31] Y. Shen, C. Li, V.C. Costa, K.L. Bray, Laser site-selective excitation spectroscopy of Eu^{3+}-doped yttrium aluminum garnet, Phys. Rev. B 68 (2003), 014101.
[32] B. Niraula, C. Rizal, Photoluminescence property of Eu^{3+} doped $CaSiO_3$ nano-phosphor with controlled grain size, Colloids Interfaces 2 (2018) 52.